

# ON THE EFFECT OF PLANETARY ROTATION ON SHEAR AND DENSITY LAYERS IN STRATIFIED FLOWS

M. GALMICHE<sup>1,2,\*</sup> and J. C. R. HUNT<sup>2</sup>

<sup>1</sup>*Department of Applied Mathematics and Theoretical Physics, University of Cambridge, Silver Street, Cambridge CB3 9EW, U.K.;* <sup>2</sup>*Department of Space and Climate Physics, University College London, 17 Gordon Street, London WC1H 0AH, U.K.*

(Received in final form 7 June 2002)

**Abstract.** The effect of the Coriolis forces on the dynamics of shear and density layers in stratified flows is investigated, an effect that has not been taken into account in most previous studies of turbulence-mean field or wave-mean field interactions. For instance, recent studies have shown that shear and density layers can grow in the presence of turbulence in a strongly stratified fluid but the effect of planetary rotation was not taken into account. To address this problem, wave-mean flow interaction in a stratified fluid is here investigated in the presence of rotation using direct numerical simulation. The results show that the wave-mean flow interaction and the formation of layers is less intense when rotation is present because the horizontal mean motions are deviated by the Coriolis forces, which tends to reduce the distortion of the wave field, and thus the wave-induced fluxes of buoyancy and momentum. This effect appears even when the rotation rate is weak.

**Keywords:** Geofluid, Rotation, Stratification, Turbulence, Wave.

## 1. Introduction

Layering processes in stratified flows involve various mechanisms, such as turbulence-mean field interactions but also wave-turbulence interactions, wave-wave interactions (Galmiche et al., 2000), wave-mean flow interactions, vortex-vortex interactions and vortex instabilities. Homogeneous, stratified turbulence has been widely investigated by Godeferd and Cambon (1994) to show that non-linear energy transfers force the tendency to anisotropy and the formation of horizontal structures. This tendency has also been observed in direct numerical simulations (e.g., Métais and Herring, 1989) and in recent stratospheric measurements (Alisse and Sidi, 2000). The anisotropic features of homogeneous turbulence can be explained by an energy transfer to Fourier modes with mainly vertical wave vectors, a mechanism that is mainly controlled by the vortex-vortex interactions (Godeferd and Cambon, 1994). A review on the dynamics of layers in geophysical flows can be found in Hunt and Galmiche (2000).

In a recent study, Galmiche et al. (2002) and Galmiche and Hunt (2002) have addressed the problem of layering in terms of turbulence-mean field interactions.

\* Address for correspondence: LEGI, BP 53, 38041 Grenoble Cedex 9, France. E-mail: Martin.Galmiche@hmg.inpg.fr



This point-of-view is different from most of the previous studies in which layers are explained in terms of anisotropy rather than in terms of vertical variability. In Galmiche et al. (2002), direct numerical simulation of freely-decaying, initially homogeneous and isotropic turbulence in the presence of a stable stratification shows that perturbations in the mean shear and mean density profiles tend to grow for short times when the stratification is strong, and remain very persistent as the turbulence evolves. This is an illustration of the property of stratified turbulence to form horizontal layers. A slightly inhomogeneous version of the Rapid Distortion Theory (Galmiche and Hunt, 2002) shows that the effects of a stratification on the wave-mean field interactions can be widely explained by the linear processes of distortion involved in the first stage of the decay of turbulence. The analytical model shows that the eddy viscosity and diffusivity associated with strongly-stratified turbulence become negative at a time of order  $N_0^{-1}$  after the beginning of turbulence decay, which accounts for the growth of the perturbations in the mean profiles. This analysis does not require any assumption on the amplitude of the perturbation field compared to the amplitude of the mean profiles but is only based on a comparison of the various timescales of the flow.

In this paper, the effect of rotation on the dynamics of layers is investigated using direct numerical simulation. In order to highlight some basic effects of the Coriolis forces, the simplified problem of wave-mean flow interaction is considered instead of the full problem of turbulence. This allows us to draw out some simple conclusions on the tendency of stratified flows to form layers when rotation is present or not.

## 2. Context of the Problem

The question addressed here is whether the interaction between a wave field and a perturbative horizontal mean flow in a stratified fluid is significantly modified by the presence of weak rotation. The presence of rotation has two main consequences on the flow dynamics. First, it has an effect on the wave field provided that the wave motion has a non-zero horizontal velocity component. Second, the horizontal mean motions are not a steady solution of the equations of motion unless they are in a geostrophic balance with the appropriate horizontal mean density gradient. In many studies, the mean flow is supposed to be in a geostrophic balance but it is assumed that the associated horizontal density gradient has no effect on the wave propagation, which is generally justified in the frame of the Boussinesq approximation (though not near critical levels). It is actually equivalent to assume that the mean flow is not in a geostrophic balance and to neglect the deviation of the mean current under the effect of rotation. However, it is probable that intermittent perturbations in the shear profile develop on a short time scale so that they should not be assumed to be in a geostrophic balance initially. In that case, the mean horizontal motions

vary slowly with time and, alternatively, can be analyzed as standing inertial waves with vertical wave vector. This is the situation we are concerned with here.

The present simulations are designed to study the sensitivity of an initial gravity wave mode with horizontal wave vector to weak,  $z$ -periodic horizontal motions. We consider here the case where the wave field and the mean flow vertical variations have the same length scale. This is a different situation from that considered in ray-tracing models in which there is a scale separation between the wave field and the mean fields. The numerical experiments are performed both in the non-rotating and rotating cases for different values of the rotation rate. The flow is relatively strongly stratified (i.e., the initial gravity wave field has low Froude number). In each case the transient interaction between the wave field and the horizontal motions is studied and particular attention is paid to the final state of the flow as a function of the rotation rate.

### 3. Theoretical Background and Numerical Methodology

We consider a three-dimensional, periodic fluid domain with periodicity  $L$  in all three directions. We use a Cartesian coordinate system  $(\mathbf{e}_1, \mathbf{e}_2, \mathbf{e}_3)$  with the  $e_3$ -direction antiparallel to the gravitational acceleration  $\mathbf{g} = -g\mathbf{e}_3$ . The spatial coordinates are denoted by  $(x, y, z) = \mathbf{x}$  and time by  $t$ . Rotation is taken into account around the vertical axis with rotation rate  $\Omega = f/2$ . The Coriolis parameter vector will be denoted by  $\mathbf{f} = f\mathbf{e}_3$ .

The velocity field is  $\mathbf{u}(\mathbf{x}, t) = (u, v, w)$  and the fluid density  $\rho(\mathbf{x}, t)$  may be decomposed as

$$\rho(\mathbf{x}, t) = \bar{\rho}(z, t) + \rho'(\mathbf{x}, t), \quad (1)$$

where  $\bar{\rho}(z, t)$  is the density averaged on a horizontal plane and  $\rho'(\mathbf{x}, t)$  is the density deviation from  $\bar{\rho}$ . The mean density profile itself may be decomposed into a linear component  $\bar{\rho}_l$  (the constant, background profile) and a  $z$ -periodic component  $\bar{\rho}_p$ :

$$\bar{\rho}(z, t) = \bar{\rho}_l(z) + \bar{\rho}_p(z, t). \quad (2)$$

The background linear profile is here supposed to be stable (i.e.,  $d\bar{\rho}_l/dz < 0$ ) and the associated Brunt–Väisälä frequency  $N$  is defined by:

$$N^2 = -\frac{g}{\rho_r} \frac{d\bar{\rho}_l}{dz}, \quad (3)$$

where  $\rho_r$  is a suitable reference density.

The density fluctuations from the background linear profile will be denoted by  $\tilde{\rho}(\mathbf{x}, t) = \rho(\mathbf{x}, t) - \bar{\rho}(z) = \bar{\rho}_p(z, t) + \rho'(\mathbf{x}, t)$ . Then, the equations of motion under the Boussinesq approximation may be written as:

$$\begin{cases} \nabla \cdot \mathbf{u} = 0 \\ \partial_t \mathbf{u} + (\mathbf{u} \cdot \nabla) \mathbf{u} + \mathbf{f} \wedge \mathbf{u} = -\rho_r^{-1} \nabla p - g (\tilde{\rho}/\rho_r) \mathbf{e}_3 + \nu \nabla^2 \mathbf{u} \\ \partial_t \tilde{\rho} + (\mathbf{u} \cdot \nabla) \tilde{\rho} = (\rho_r/g) N^2 w + \kappa \nabla^2 \tilde{\rho} \end{cases} \quad (4)$$

where  $\nabla = (\partial_x, \partial_y, \partial_z)$ ,  $p$  is the pressure deviation from the hydrostatic profile,  $\nu$  is the kinematic viscosity and  $\kappa$  is the thermal diffusivity of the fluid.

Stratified, rotating flows are simulated from specified initial conditions thanks to a pseudo-spectral code (see Thual, 1992) with fully periodic boundary conditions and  $64^3$  grid points.

The equations of motion are solved using a poloidal–toroidal decomposition of the velocity field that we may introduce here briefly. One can show (see Thual, 1992) that an alternative description of *any* solenoidal velocity field  $\mathbf{u} = (u, v, w)$  with periodic boundary conditions is provided by the knowledge of:

- (i)  $w(\mathbf{x}, t)$ , the vertical velocity,
- (ii)  $\partial_x v - \partial_y u = \zeta(\mathbf{x}, t)$ , the vertical vorticity and
- (iii)  $\bar{\mathbf{u}}(z, t) = \bar{u}(z, t) \mathbf{e}_1 + \bar{v}(z, t) \mathbf{e}_2$ , the horizontal mean flow (i.e., the horizontal velocity field averaged on a horizontal plane).

Using the  $w$ - $\zeta$ - $\bar{\mathbf{u}}$  decomposition, the equations of motion become:

$$\begin{cases} \nabla \cdot \mathbf{u} = 0 \\ \partial_t \nabla^2 w - \nabla \wedge (\nabla \wedge [(\mathbf{u} \cdot \nabla) \mathbf{u}]) \cdot \mathbf{e}_3 + f \partial_z \zeta = -(g/\rho_r) \nabla_H^2 \tilde{\rho} + \nu \nabla^4 w \\ \partial_t \zeta + \nabla \wedge [(\mathbf{u} \cdot \nabla) \mathbf{u}] \cdot \mathbf{e}_3 - f \partial_z w = \nu \nabla^2 \zeta \\ \partial_t \bar{u} + \partial_z \langle uw \rangle^{xy} - f \bar{v} = \nu \partial_{zz} \bar{u} \\ \partial_t \bar{v} + \partial_z \langle vw \rangle^{xy} + f \bar{u} = \nu \partial_{zz} \bar{v} \\ \partial_t \tilde{\rho} + (\mathbf{u} \cdot \nabla) \tilde{\rho} = (\rho_r/g) N^2 w + \kappa \nabla^2 \tilde{\rho} \end{cases} \quad (5)$$

where  $\nabla_H = (\partial_x, \partial_y, 0)$ . As in the present study fully periodic boundary conditions are used for the velocity field, the mean flow profile is also  $z$ -periodic and there is no uniform background shear.

In the numerical procedure, all variables  $w(\mathbf{x}, t)$ ,  $\zeta(\mathbf{x}, t)$ ,  $\bar{u}(z, t)$ ,  $\bar{v}(z, t)$ , and  $\tilde{\rho}(\mathbf{x}, t)$  are Fourier-transformed and the Equation (5) is solved in the Fourier space, except when computing the non-linear terms that are calculated in the physical space. A second-order, *slaved-frog* temporal scheme (see Frisch et al., 1986) is used.

It is useful to make the connection between the  $w$ - $\zeta$ - $\bar{\mathbf{u}}$  decomposition and the often-used poloidal–toroidal decomposition (see, for instance, Riley and Lelong, 2000):

$$\mathbf{u}(\mathbf{x}, t) = \bar{\mathbf{u}}(z, t) + \mathbf{u}_{\text{pol}}(\mathbf{x}, t) + \mathbf{u}_{\text{tor}}(\mathbf{x}, t). \quad (6)$$

Here the poloidal and toroidal velocities are defined by:

$$\mathbf{u}_{\text{pol}}(\mathbf{x}, t) = \nabla \wedge [\nabla \wedge E(\mathbf{x}, t) \mathbf{e}_3] \quad \text{and} \quad \mathbf{u}_{\text{tor}}(\mathbf{x}, t) = \nabla \wedge [B(\mathbf{x}, t) \mathbf{e}_3], \quad (7)$$

where functions  $E$  and  $B$  are such that  $w = -\nabla_H^2 E$  and  $\zeta = -\nabla_H^2 B$ . The poloidal component  $\mathbf{u}_{\text{pol}}$  has zero vertical vorticity and the toroidal component  $\mathbf{u}_{\text{tor}}$  has zero vertical velocity. In the linear limit, the poloidal component may be seen as the wave part of the velocity field and the toroidal component may be seen as the turbulent (or 'vortical') part of the velocity field.

As the computation domain is periodic, the kinetic energy per unit mass averaged over the box may be written as:

$$E_{\text{kin}}(t) = E_{\bar{u}}(t) + E_{\bar{v}}(t) + E_{\text{pol}}(t) + E_{\text{tor}}(t), \quad (8)$$

where  $E_{\bar{u}}(t) = (1/2)\langle \bar{u}^2 \rangle^z$  (respectively  $E_{\bar{v}}(t) = (1/2)\langle \bar{v}^2 \rangle^z$ ) is the energy of the  $x$ -component (respectively the  $y$ -component) of the mean flow,  $E_{\text{pol}}(t) = (1/2)\langle \mathbf{u}_{\text{pol}}^2 \rangle^{xyz}$  is the poloidal energy and  $E_{\text{tor}}(t) = (1/2)\langle \mathbf{u}_{\text{tor}}^2 \rangle^{xyz}$  is the toroidal energy. Here,

$$\langle \cdot \rangle^z = \frac{1}{L} \int_0^L \cdot dz \quad \text{and} \quad \langle \cdot \rangle^{xyz} = \frac{1}{L^3} \int_0^L \int_0^L \int_0^L \cdot dx dy dz. \quad (9)$$

The total mean flow energy will be denoted by  $E_{sh} = E_{\bar{u}} + E_{\bar{v}}$ .

Taking the linear stratification  $\bar{\rho}_l$  as the reference state, the potential energy may be written as:

$$E_{\text{pot}}(t) = E_{\bar{\rho}}(t) + E_{\rho'}(t), \quad (10)$$

where  $E_{\bar{\rho}}(t) = (1/2)(g/\rho_r N)^2 \langle \bar{\rho}_p^2 \rangle^z$  is the energy stored in the density periodic mean profile and  $E_{\rho'}(t) = (1/2)(g/\rho_r N)^2 \langle \rho'^2 \rangle^{xyz}$  is the *fluctuating* potential energy.

The total\* energy  $E(t)$  in the box at time  $t$  is then

$$E(t) = E_{\text{kin}}(t) + E_{\text{pot}}(t). \quad (11)$$

The 'total' energy of the wave field at time  $t$  may be defined as

$$E_{\text{wave}}(t) = E_{\text{pol}}(t) + E_{\rho'}(t). \quad (12)$$

\* Here the word 'total' has to be understood in the mechanical sense ('kinetic plus potential'), not the thermodynamical sense.

#### 4. The Numerical Experiments

The initial condition is a wave mode with amplitude  $w_0$  and vertical phase planes (i.e., purely vertical velocity fluctuations) perturbed by a weak mean flow mode in the  $x$ -direction with amplitude  $\bar{u}_0 \ll w_0$ . Note that the wave mode is an exact solution of the equations of motion (when no mean flow is present) with or without rotation since for this mode  $\mathbf{f} \wedge \mathbf{u} = 0$ .

The stratification is initially uniform (i.e.,  $\bar{\rho}_p(z, 0) = 0$ ) with density profile  $\bar{\rho}_l(z)$  and Brunt–Väisälä frequency  $N$  defined by (3).

The wave mode has wavenumber  $2\pi/L$  and the associated velocity and density fields are

$$\begin{cases} w(\mathbf{x}, 0) = w_0 \cos(2\pi x/L) \\ \tilde{\rho}(\mathbf{x}, 0) = \tilde{\rho}_0 \sin(2\pi x/L), \end{cases} \quad (13)$$

where  $\tilde{\rho}_0 = (\rho_r/g)Nw_0$ . The phase velocity of this wave mode is  $NL/2\pi \mathbf{e}_1$ .

The perturbative mean flow is given by:

$$\bar{u}(z, 0) = \bar{u}_0 \cos(2\pi z/L) \quad (14)$$

and  $\bar{v}(z, 0) = 0$ . Note that in the absence of a wave field and dissipation, the time-evolution for  $t > 0$  of  $\bar{u}(z, t)$  and  $\bar{v}(z, t)$  would be given by the following exact solution of the equations of motion:

$$\begin{cases} \bar{u}(z, t) = \bar{u}_0 \cos(2\pi z/L) \cos ft \\ \bar{v}(z, t) = -\bar{u}_0 \cos(2\pi z/L) \sin ft, \end{cases} \quad (15)$$

which, when  $f \neq 0$ , corresponds to a standing inertial wave with frequency  $f$ , i.e., the superposition of two inertial waves with wave vectors  $(2\pi/L)\mathbf{e}_3$  and  $-(2\pi/L)\mathbf{e}_3$ .

Note that from this initial condition, a shear time scale  $\alpha^{-1}$  may be defined, where  $\alpha = \bar{u}_0/L$ .

The wave and mean flow amplitudes, the initial stratification, the size of the periodic box and the properties of the fluid are such that  $Fr = w_0/NL = 0.1$ ,  $Re = w_0L/\nu = 330$  and  $E_{\bar{\pi}}(0)/E_{\text{wave}}(0) = 0.1$  (weak mean flow profile). This implies that the wave motions are initially weak compared to the intensity of the stratification, but large compared to the amplitude of the mean flow mode.

The Prandtl number is  $Pr = \nu/\kappa = 1$  and four values of the rotation rate are considered:  $f/N = 0$  (Simulation A), 0.01 (Simulation B), 0.03 (Simulation C) and 0.05 (Simulation D).

The rotation rate may also be quantified by a Rossby number defined as:

$$Ro = \frac{\bar{u}_0}{fL}. \quad (16)$$

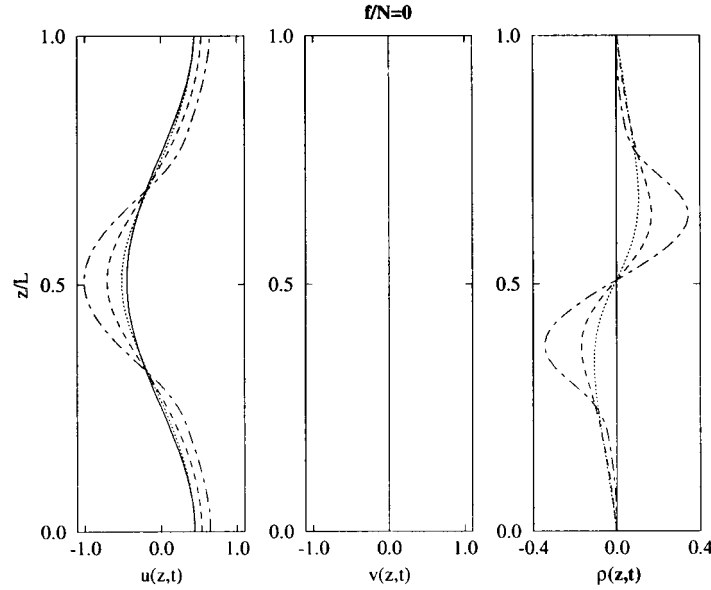


Figure 1. Profiles of  $\bar{u}$ ,  $\bar{v}$  and  $\bar{\rho}_p$  in Simulation A ( $f/N = 0$ ) at  $Nt = 0$  (solid line),  $Nt = 10$  (dot-dashed line),  $Nt = 30$  (dashed line) and  $Nt = 50$  (dotted line). The horizontal mean flow is first accelerated in the  $x$ -direction and then slowly decays. The transverse component  $\bar{v}(z, t)$  of the horizontal mean flow remains zero. Variations are generated in the mean density profile  $\bar{\rho}(z, t)$  and then slowly decay but remain significant at large time.

The values of the inverse Rossby number are then  $Ro^{-1} = 0$  (Simulation A), 0.2 (Simulation B), 0.6 (Simulation C) and 1 (Simulation D). The results of the numerical experiments are presented here and discussed in Section 5.

The profiles of  $\bar{u}(z, t)$ ,  $\bar{v}(z, t)$  and  $\bar{\rho}_p(z, t)$  are plotted at  $Nt = 0$ ,  $Nt = 10$ ,  $Nt = 30$  and  $Nt = 50$  on Figure 1 (simulation A), Figure 2 (simulation B), Figure 3 (simulation C) and Figure 4 (simulation D). The time evolution of some global quantities are plotted on Figures 5 to 8 for each simulation: energy of the mean flow  $E_{sh}(t)$  (Figure 5), energy of the vertical density structure  $E_{\bar{\rho}}(t)$  (Figure 6), energy of the poloidal velocity component  $E_{pol}(t)$  (Figure 7), energy of the density fluctuations  $E_{\rho'}(t)$  (Figure 8) and energy of the toroidal motions  $E_{tor}(t)$  (Figure 9). In these perturbed stratified rotating flows, it is also interesting to quantify how the wave activity is distributed between kinetic and potential energy. The time evolution of the ratio  $E_{\rho'}(t)/E_w(t)$  (where  $E_w(t)$  is the energy associated with the vertical velocity fluctuations) is plotted on Figure 10 for each simulation.

In order to illustrate the effect of rotation on the wave-mean interaction, the final value (at  $t = T_f = 80N^{-1}$ ) of energies  $E_{sh}$ ,  $E_{\bar{\rho}}$  and  $E_{wave}$  are plotted on Figures 11, 12 and 13 respectively as a function of the rotation rate. On these plots, the magnitude of the rotation rate is given in terms of the inverse Rossby number defined by (16).

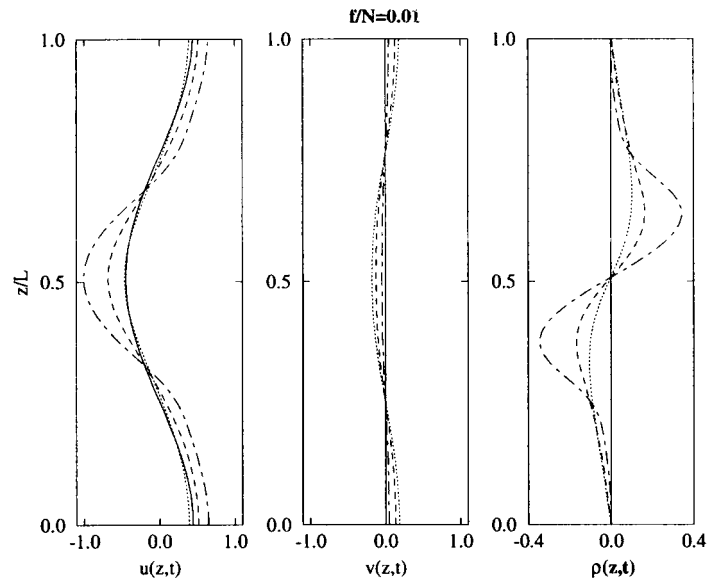


Figure 2. Profiles of  $\bar{u}$ ,  $\bar{v}$  and  $\bar{\rho}_p$  in Simulation B ( $f/N = 0.01$ ) at  $Nt = 0$  (solid line),  $Nt = 10$  (dot-dashed line),  $Nt = 30$  (dashed line) and  $Nt = 50$  (dotted line). In this simulation with very low rotation rate, the results are not significantly changed compared to the non-rotating case (Simulation A), although the horizontal mean flow is slightly deviated towards the transverse direction ( $\bar{v} \neq 0$ ).

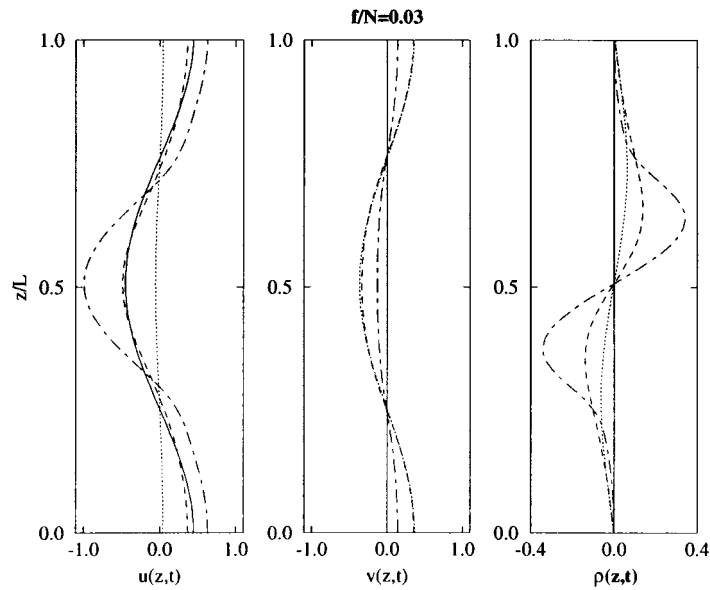


Figure 3. Profiles of  $\bar{u}$ ,  $\bar{v}$  and  $\bar{\rho}_p$  in Simulation C ( $f/N = 0.03$ ) at  $Nt = 0$  (solid line),  $Nt = 10$  (dot-dashed line),  $Nt = 30$  (dashed line) and  $Nt = 50$  (dotted line). The horizontal mean flow is deviated towards the transverse direction and the final variations in the mean density profile are significantly smaller than in the non-rotating case (Simulation A).

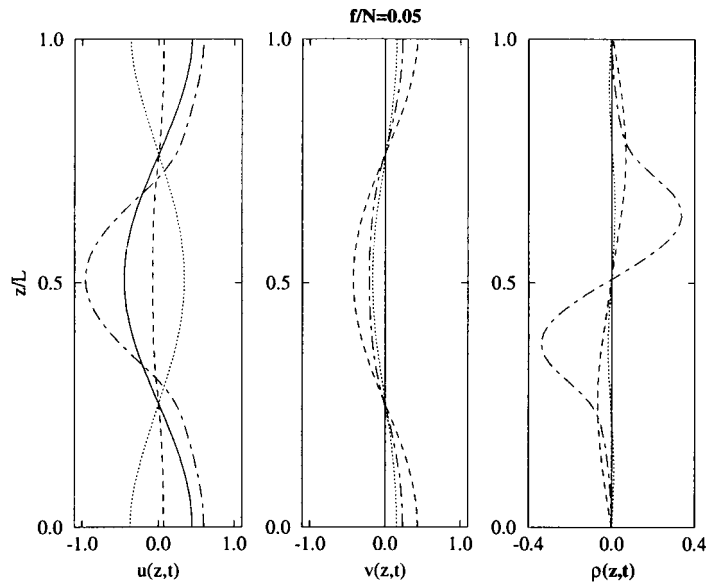


Figure 4. Profiles of  $\bar{u}$ ,  $\bar{v}$  and  $\bar{\rho}_p$  in Simulation D ( $f/N = 0.05$ ) at  $Nt = 0$  (solid line),  $Nt = 10$  (dot-dashed line),  $Nt = 30$  (dashed line) and  $Nt = 50$  (dotted line). The horizontal mean flow is strongly affected by the Coriolis forces which induces oscillations of the direction of the mean velocity. The vertical variations in the final mean density profile are almost zero.

## 5. Discussion

In the absence of rotation (Simulation A), the horizontal mean flow keeps a constant direction ( $\bar{v}(z, t) = 0$  at any time) and changes amplitude as a consequence of the wave-mean flow interaction but the flow field remains two-dimensional (Figure 1). The mean flow first accelerates ( $E_{sh} \simeq 3.5E_{sh}(0)$  at  $Nt = 10$ ) and then decays with weak oscillations on a time scale of order  $\alpha^{-1} = L/\bar{u}_0$  (see Figure 5, solid line). During the wave-mean flow interaction, the mean density profile is also significantly affected as a result of the wave-induced buoyancy flux (Figure 1 and Figure 6, solid line). The potential energy associated with the vertical variations of  $\bar{\rho}$  is maximum at  $Nt = 10$  and then decreases slowly with weak oscillations but remains significant at large times. As a counterpart to the growth in the mean profiles, the kinetic and potential energies  $E_{pol}$  and  $E_{\rho'}$  associated with the wave field decrease rapidly (Figures 7 and 8, solid line).

In the rotating simulation with smallest rotation rate (Simulation B,  $f/N = 0.01$ ), the results are not significantly changed although the horizontal mean flow is affected by the Coriolis forces and is slightly deviated into the transverse direction  $y$  ( $\bar{v} \neq 0$ , Figure 2). However, the effects of rotation become crucial in Simulations C ( $f/N = 0.03$ ) and D ( $f/N = 0.05$ ). In these simulations, the horizontal mean flow is largely deviated into the transverse direction under the effect of the Coriolis forces. The short-time acceleration of the mean flow ( $t < 10N^{-1}$ ) is similar to

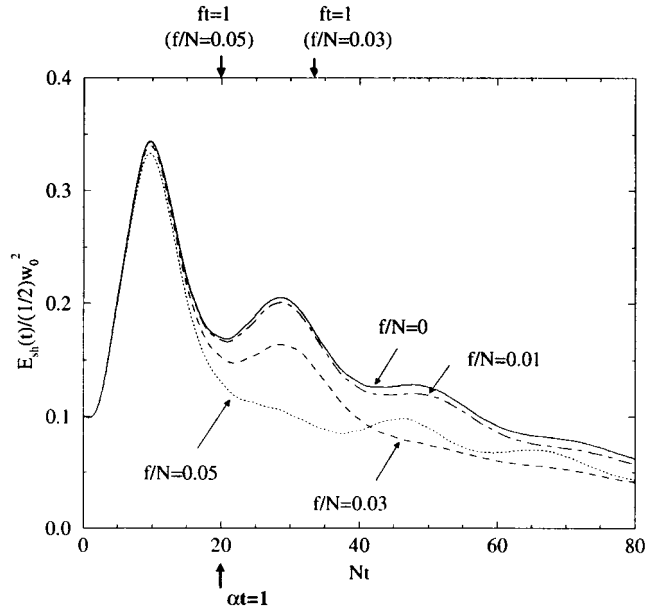


Figure 5. Evolution of the energy of the horizontal mean motions  $E_{sh} = E_{\bar{u}} + E_{\bar{v}}$  as a function of  $Nt$  in Simulations A ( $f/N = 0$ , solid line), B ( $f/N = 0.01$ , dot-dashed line), C ( $f/N = 0.03$ , dashed line) and D ( $f/N = 0.05$ , dotted line). In all cases the mean flow energy first increases and then slowly decreases with some more or less persistent oscillations. However, the wave-mean flow interaction is more intense and the decay of  $E_{sh}(t)$  is much slower in the non-rotating case (Simulation A).

that observed without rotation but the subsequent decay is much faster in both Simulations C and D. Similarly, the potential energy associated with the variations in the mean density profile decays more rapidly than in the non-rotating case for  $t > 20N^{-1}$ .

It is clear in Figures 11 to 13 how the presence of rotation changes the wave-mean flow interaction and thus the behaviour of the mean fields. The final values of  $E_{sh}$  and  $E_{\bar{p}}$  are maximum for  $Ro^{-1} = 0$  (Simulation A). When the Rossby number is of order unity (Simulations C and D), the final energy of the mean horizontal motions is about 35% less and the final potential energy associated with the vertical density structure is roughly zero. The final energy of the wave field is minimum in the non-rotating case and is about 30% more when the Rossby number is of order unity.

The toroidal energy plotted on Figure 9 quantifies the energy of wave motions with non-zero vertical vorticity and may be seen as a measure of the effect of the Coriolis forces on the wave field.

A variety of mechanisms are involved in these numerical experiments, which we may summarize here as follows:

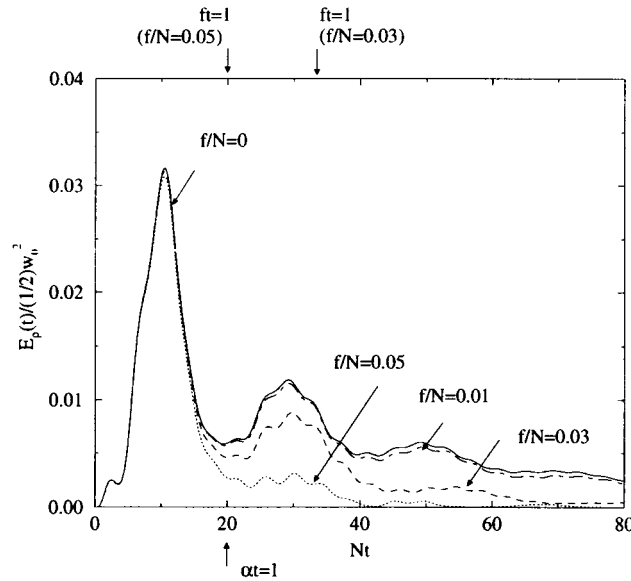


Figure 6. Evolution of the energy of the vertical density structure  $E_{\overline{\rho}}$  as a function of  $Nt$  in Simulations A ( $f/N = 0$ , solid line), B ( $f/N = 0.01$ , dot-dashed line), C ( $f/N = 0.03$ , dashed line) and D ( $f/N = 0.05$ , dotted line). The short-time increase of  $E_{\overline{\rho}}$  is followed by a decay that is faster as the rotation rate is increased. The final value of  $E_{\overline{\rho}}$  is roughly zero in the simulation with highest rotation rate (Simulation D).

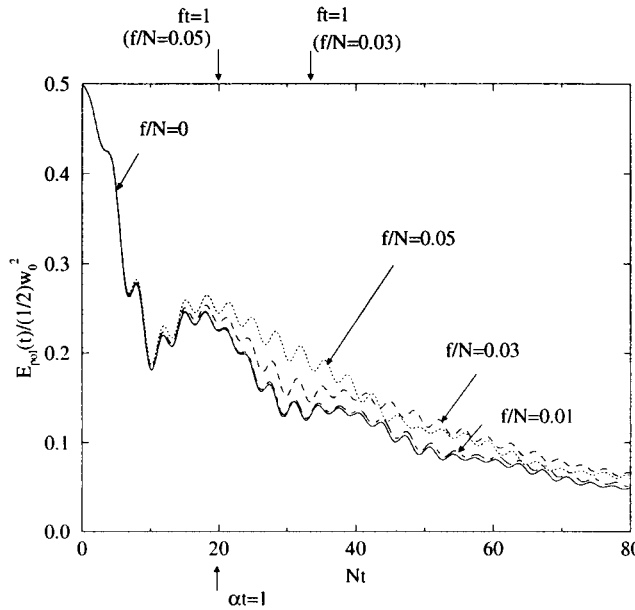


Figure 7. Evolution of the poloidal energy  $E_{\text{pol}}$  as a function of  $Nt$  in Simulations A ( $f/N = 0$ , solid line), B ( $f/N = 0.01$ , dot-dashed line), C ( $f/N = 0.03$ , dashed line) and D ( $f/N = 0.05$ , dotted line). The wave motions decay in all cases as the wave-mean flow interaction goes on but remain more active at large time when rotation is present.

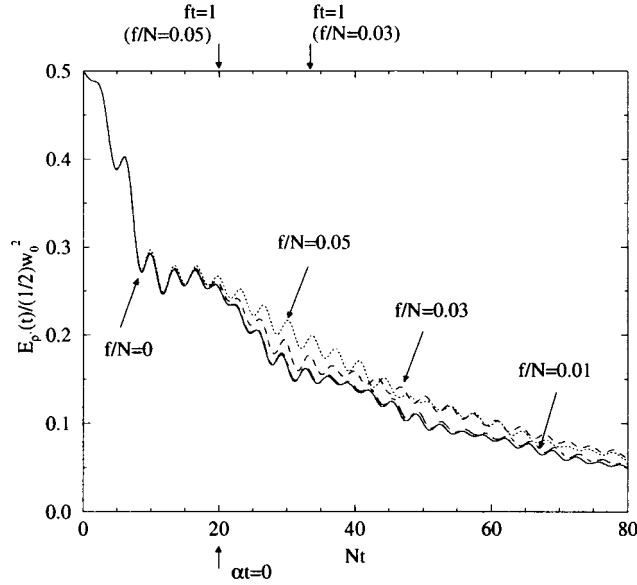


Figure 8. Evolution of the energy of the density fluctuations  $E_{\rho'}$  as a function of  $Nt$  in Simulations A ( $f/N = 0$ , solid line), B ( $f/N = 0.01$ , dot-dashed line), C ( $f/N = 0.03$ , dashed line) and D ( $f/N = 0.05$ , dotted line). Associated with wave motions, the density fluctuations decay but are more persistent at large time when rotation is present.

- (i) Initially, the wave vector of the wave mode and the horizontal mean flow have the same direction. Thus, for short times, the wave field is distorted by the mean shear on a time scale of order  $\alpha^{-1}$ .
- (ii) The velocity field is distorted by the effect of the stratification on a time scale of order  $N^{-1}$ .
- (iii) The wave field and the mean fields exchange energy.
- (iv) The horizontal mean flow is deviated on a time scale of order  $f^{-1}$ .

The effect (i) of distortion by the mean shear, together with the effect (ii) of the restoring buoyancy forces, have been studied by Galmiche and Hunt (2002) in the case of an initially homogeneous and isotropic velocity field with strong stratification, weak shear and no rotation. This is a different situation from that considered here with weak rotation and only one wave mode in the initial condition. However, the resulting effects of the momentum and buoyancy fluxes on the mean flow and density fields are similar to those described in the frame of the Rapid Distortion Theory for short time and strong stratification. The mean flow perturbation grows on a time scale of order  $N^{-1}$  (Figure 5) and variations in the mean density profile develop on the same time and length scales (Figure 6). A similar coupling between the mean density and mean velocity field has been described analytically by Galmiche and Hunt (2002). The present simulations not only confirm this short-time tendency but also show that it is not significantly affected by weak rotation.

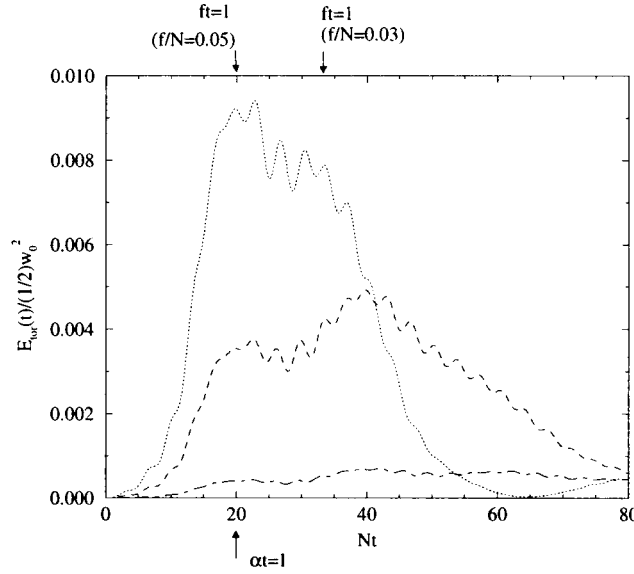


Figure 9. Evolution of the toroidal energy  $E_{\text{tor}}$  as a function of  $Nt$  in Simulations A ( $f/N = 0$ , solid line), B ( $f/N = 0.01$ , dot-dashed line), C ( $f/N = 0.03$ , dashed line) and D ( $f/N = 0.05$ , dotted line). The toroidal energy is zero in the non-rotating case because the flow remains two-dimensional. When rotation is present (Simulations B, C and D), the Coriolis forces become significant when the wave field starts to be distorted by the mean shear, inducing  $\mathbf{f} \wedge \mathbf{u} \neq 0$ . This produces toroidal wave motions, i.e., motions with non-zero vertical vorticity. However, the production of toroidal motions is strongly reduced after a time scale of order  $f^{-1}$  because the horizontal mean flow is deviated into the transverse direction  $y$ . This reduces the distortion of the wave field, the intensity of the horizontal velocity fluctuations, the effect of the Coriolis forces and, therefore, the intensity of the toroidal motions.

This is not unexpected as the flow field is affected by the Coriolis forces on a time scale of order  $f^{-1} \gg N^{-1}$  in all simulations.

The large-time ( $Nt \sim \alpha^{-1} > 10N^{-1}$ ) behaviour of the mean profiles is found to be controlled by the shear time scale rather than the buoyancy time scale (see Figures 5 and 6). The energy transfers (iii) between the wave field and the mean fields occur on a time scale  $\alpha^{-1}$  and lead to some more or less persistent oscillations of  $E_{sh}$  and  $E_{\bar{p}}$  in the non-rotating simulations as well as in the rotating simulations. This large-time behaviour could not be described in the Rapid Distortion model of Galmiche and Hunt (2002), which was only valid for  $Nt \sim 1$ .

The deviation of the mean flow (iv) under the effect of the Coriolis forces starts to have an effect on the flow dynamics once the angle  $\Theta$  between the horizontal mean flow direction and the horizontal wave vector of the wave field becomes significant. The distortion of the wave field is maximum when  $\Theta$  is zero, and tends to zero when  $\Theta$  tends to  $\pi/2$ . The time  $t_0$  at which  $\Theta = \pi/2$  may be estimated using the solution (15). This solution is only valid in the absence of a wave field

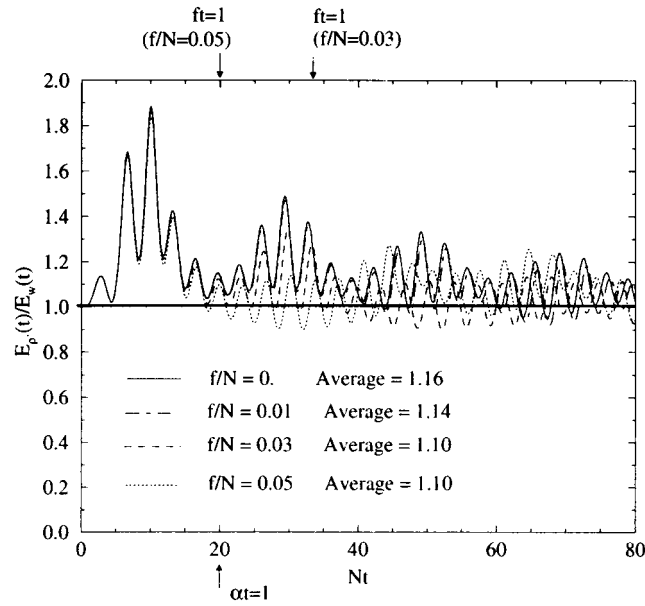


Figure 10. Ratio of potential wave energy to vertical fluctuations energy as a function of  $Nt$  and average value in Simulations A ( $f/N = 0$ , solid line), B ( $f/N = 0.01$ , dot-dashed line), C ( $f/N = 0.03$ , dashed line) and D ( $f/N = 0.05$ , dotted line). As the rotation rate is increased, the wave field becomes closer to the potential-kinetic equipartition due to the damping of the wave-mean flow interaction.

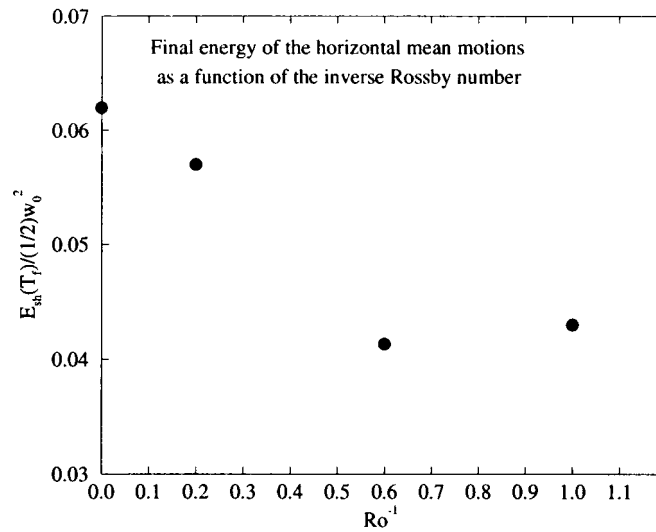


Figure 11. Final energy of the horizontal mean motions  $E_{sh}(T_f) = E_{\bar{u}}(T_f) + E_{\bar{v}}(T_f)$  as a function of the inverse Rossby number ( $T_f = 80N^{-1}$ ). The enhancement of the horizontal mean motions is damped by the presence of rotation.

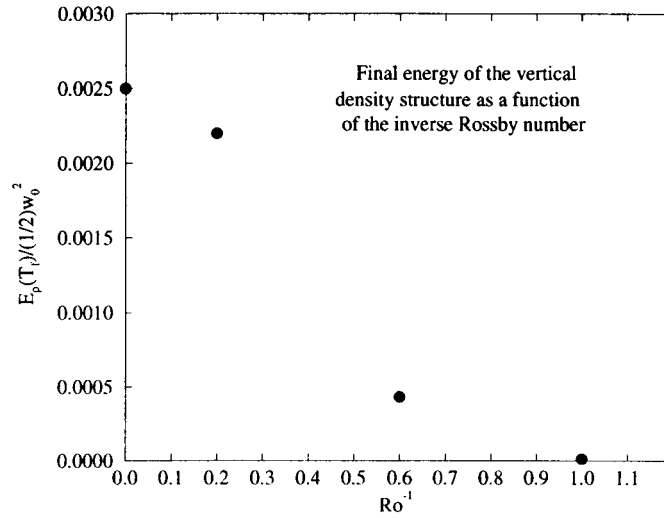


Figure 12. Final energy of the vertical density structure  $E_{\bar{\rho}}(T_f)$  as a function of the inverse Rossby number ( $T_f = 80N^{-1}$ ). The development of variations in the mean density profile is strongly reduced when rotation is present.

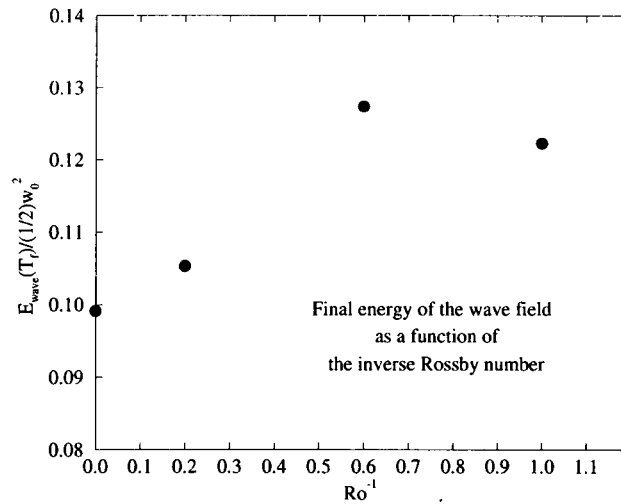


Figure 13. Final energy of the wave field  $E_{\text{wave}}(T_f)$  as a function of the inverse Rossby number ( $T_f = 80N^{-1}$ ). The wave field is more persistent as the rotation rate is increased.

but is still a good estimation as far as the direction (but not the amplitude) of the mean flow is concerned. This leads to  $ft_0 = \pi/2$ .

In the rotating simulation with lower rotation rate (Simulation B),  $t_0$  is much larger than any time scale of the flow. In particular,  $t_0 \gg \alpha^{-1}$ . Thus, the wave-mean flow interaction has time to develop before the effect of the mean flow deviation becomes significant, and no significant difference is observed compared

to the non-rotating simulation. However, we have  $t_0 \simeq 0.9\alpha^{-1}$  in Simulation C and  $t_0 \simeq 1.6\alpha^{-1}$  in Simulation D. Thus, the deviation of the mean flow becomes significant on the same time scale as that of the wave-mean flow interaction. As  $\Theta$  goes to  $\pi/2$ , the distortion of the wave field becomes less and less efficient and the wave-mean flow interaction is reduced. This mechanism is particularly significant in Simulation D where  $f = \alpha$ , i.e.,  $Ro = 1$ , which is illustrated by the low final values of  $E_{sh}$  and  $E_{\bar{p}}$  (Figures 11 and 12). On the other hand, the wave field is less affected by the mean flow so that its final energy is higher than in the non-rotating simulations (Figure 13).

The reduction of the distortion process in the rotating experiments has also an effect on the properties of the wave field, in particular on the ratio  $E_{\rho'}/E_w$ . This ratio is unity initially as for any purely vertical wave motions. Figure 10 shows that in the non-rotating simulation,  $E_{\rho'}/E_w$  oscillates but is mainly greater than unity during the experiment (solid line). This is due to the wave-mean flow interaction, which reduces the amplitude of the vertical velocity fluctuations. The time-averaged value of  $E_{\rho'}/E_w$  is about 1.16. When rotation is present, however, the time-averaged value of  $E_{\rho'}/E_w$  is closer to unity (1.1 in Simulation D) due to the reduction of the wave-mean flow interaction. This result has some practical importance as an estimation of  $E_{\rho'}/E_w$  is needed in models of atmospheric or oceanic flows. The present results suggest that the wave field is closer to the potential-kinetic equipartition when the wave-mean flow interaction is reduced by the effects of rotation.

The effect of rotation on the wave field is also clear on Figure 9. The time-evolution of the toroidal energy is easy to interpret in the framework of the above-described scenario. When there is no rotation, the flow remains two-dimensional,\* implying  $E_{\text{tor}}(t) = 0$ . When rotation is present, the Coriolis forces start to affect the wave field once the effect of distortion becomes significant, producing horizontal velocity fluctuations, i.e., after a time scale of order  $\alpha^{-1}$ . However, as the horizontal mean motions are deviated by the Coriolis forces, the distortion of the wave field is reduced and the toroidal motions stop growing. They actually decay and are weak at the end of the simulations.

The results from these numerical simulations suggest some new concepts on the behaviour of layers in stratified rotating flows. They may be interpreted in terms of the sensitivity of wave motions to relatively weaker horizontal mean motions. This approach contrasts with the classical linear stability analysis, where generally the ‘mean’ is supposed to be large and the ‘fluctuating’ is supposed to be small, but is similar to the approach of Galmiche et al. (2002) and Galmiche and Hunt (2002) of ‘weakly-modulated’, strongly-stratified turbulence. The main difference here is that strong anisotropy is present in the initial condition since only one wave mode is present initially.

\* Note that in some other situations with higher Reynolds number or larger mean flow amplitude, the flow may be sensitive to three-dimensional perturbations.

In real flows, intermittent perturbations of the vertical mean shear are ubiquitous. These perturbations may appear on a short time scale and therefore, in the presence of rotation, may not be in a geostrophic balance. They may rather be small-amplitude inertial waves, as in the present simulations. Our results show that in that case, the presence of weak rotation reduces significantly the growth of perturbations in the mean flow and density profile, which is generally observed in strongly-stratified flows. The deviation (and oscillations when the rotation rate is large enough) of the horizontal mean motions prevent the wave field and the mean flow from interacting permanently. This happens even for low rotation rate  $f$ , provided that the mean flow amplitude  $\bar{u}_0$  is not too large so that  $Ro = \bar{u}_0/fL \sim 1$  (here  $L$  is the vertical length scale of the mean flow mode). This may reduce significantly the tendency of strongly-stratified flows to form horizontal layers. We note that this conclusion is also consistent with spectral approaches of energy transfers in stratified flows, which show that in the presence of rotation, the energy-containing modes tend to have more horizontal wave vectors (Godefert and Cambon, 1994).

The results may be changed for higher rotation rates. When  $f$  is of the order or lower than  $\alpha$ , as in the present simulations, the deviation  $\Theta$  of the mean flow does not largely exceed  $\pi/2$  during the wave-mean flow interaction. For large time, the mean flow keeps changing direction under the effect of rotation but its amplitude is no more significantly affected by the wave field whose amplitude is low. However, when  $f \gg \alpha$ , the wave field may remain active while the direction of the horizontal mean motions oscillates quickly. This may produce an intermittent wave-mean flow interaction, on a time scale of order  $f^{-1}$ .

## 6. Conclusion

Direct numerical simulations showed some detailed effects of rotation on wave motions in a stratified fluid. The sensitivity of initially purely vertical wave motions to a small-amplitude horizontal mean flow mode has been studied in the non-rotating and rotating cases for different values of the rotation rate ( $f/N$  from 0 to 0.05). The simulations show that in the absence of rotation, pure vertical wave motions are very sensitive to weak horizontal mean motions. The wave-mean flow interaction leads to distortion and energy input into the mean flow even though this mechanism is slow when the initial mean flow is weak initially. The presence of rotation strongly modifies this mechanism even when the rotation rate is much less than the buoyancy frequency. The Coriolis effects reduce the wave-mean flow interaction because the deviation of the horizontal mean flow induces changes in the angle  $\Theta$  between the horizontal wavevector of the wave field and the direction of the horizontal mean flow. Therefore, the distortion of the wave field is reduced and the wave-mean flow interaction is less intense. An important implication is that the mean density structure is also much less affected in the rotating case than in the

non-rotating case. The variability in the final mean shear and mean density profiles was found to be minimum when the initial flow field has  $Ro \sim 1$ , i.e., when the time scale associated with mean shear flow is of the order of  $f^{-1}$ . The wave-mean flow interaction is reduced in that case because oscillations of  $\Theta$  take place on a time scale that is of the order of the time scale of the energy transfers between the wave field and the mean flow. This illustrates the limiting effect of weak rotation on the formation of horizontal ‘density layers’ in stratified fluids.

These preliminary simulations open the way to further investigations of transient wave-mean flow interactions in stratified rotating flows. Even in elementary numerical experiments with simple initial conditions, many control parameters can be changed and may have a great effect on the initial-value problem. In particular, large-amplitude mean flows may lead the wave field to criticality and cause complex mechanisms such as wave breaking and turbulent mixing. On the other hand, large-amplitude vertical wave motions (i.e., wave motions at high Froude number) are strongly affected by small-amplitude mean flows. This interaction may be slow but lead the wave field to overturning, turbulence and dramatic change in the dissipation rate. Also, it would be of interest to study the wave-mean flow interaction when the two initial modes have different space periodicity. This would of course involve more small-scale processes and require higher resolution.

### Acknowledgements

M.G. acknowledges the support from grants awarded by the Meteorological Office to the Department of Space and Climate Physics, University College London, and from the Newton Trust to the Department of Applied Mathematics and Theoretical Physics, University of Cambridge. We are grateful for many useful conversations on these flow problems from many colleagues, especially G. J. Shutts, M. E. McIntyre, C. Souprayen, C. Vassilicos, C. D. Warner, H. J. S. Fernando, P. A. Durbin and O. Thual. Our simulations have been performed thanks to a numerical code originally developed by O. Thual.

### References

- Alisse, J.-R. and Sidi, C.: 2000, ‘Experimental Probability Density Functions of Small-Scale Fluctuations in the Stably Stratified Atmosphere’, *J. Fluid Mech.* **402**, 137–162.
- Frisch, U., Su She, Z., and Thual, O.: 1986, ‘Viscoelastic Behaviour of Cellular Solutions to the Kuramoto–Sivashinsky Model’, *J. Fluid Mech.* **168**, 221–240.
- Galmiche, M. and Hunt, J. C. R.: 2002, ‘The Formation of Shear and Density Layers in Stably-Stratified Turbulent Flows: Linear Processes’, *J. Fluid Mech.* **455**, 243–262.
- Galmiche, M., Thual, O., and Bonneton, P.: 2000, ‘Wave/Wave Interaction Producing Horizontal Mean Flows in Stably Stratified Fluids’, *Dyn. Atmos. Oceans* **31**, 193–207.
- Galmiche, M., Thual, O., and Bonneton, P.: 2002, ‘Direct Numerical Simulation of Turbulence Mean Field Interactions in a Stably-Stratified Fluid’, *J. Fluid Mech.* **455**, 213–242.

- Godeferd, F. S. and Cambon, C.: 1994, 'Detailed Investigation of the Energy Transfers in Homogeneous Stratified Turbulence', *Phys. Fluids* **6**, 2084–2100.
- Hunt, J. C. R. and Galmiche, M.: 2000, 'Dynamics of Layers in Geophysical Flows', in J. L. Limley (ed.), *Fluid Mechanics and the Environment: Dynamical Approaches, A Symposium in Honor of Sid Leibovitch on his 60th Birthday, Cornell University, August 1999*, pp. 121–150.
- Métais, O. and Herring, J. R.: 1989, 'Numerical Simulations of Freely Evolving Turbulence in Stably Stratified Fluids', *J. Fluid Mech.* **202**, 117–148.
- Riley, J. J. and Lelong, M. P.: 1999, 'Fluid Motion in the Presence of Strong Stable Stratification', *Annu. Rev. Fluid Mech.* **32**, 613–657.
- Thual, O.: 1966, 'Zero-Prandtl Number Convection', *J. Fluid Mech.* **240**, 229–258.

